Crossover to an Even-Parity Lowest Excited Singlet in Large Oligorylenes: A Theoretical Study

Stoyan Karabunarliev,*,† Martin Baumgarten,‡,§ and Klaus Müllen‡

Department of Physics, Bourgas University of Technology, 8010 Bourgas, Bulgaria, and Max-Planck-Institut für Polymerforschung, Ackermannweg 10, D-55128 Mainz, Germany

Received: March 12, 1998; In Final Form: June 8, 1998

The series of oligorylenes from perylene to pentarylene are theoretically studied with the purpose to predict the dipole character of the lowest excited singlet state, S_1, for the larger oligomers and the polymer. Like polyenes and other extended conjugated systems, oligorylenes have two low-lying excited singlet states of odd (B_{3u}) and even (A_g) parity whose relative ordering determines the nature of the basic photoexcitation processes. The equilibrium geometries of oligorylenes in the ground and excited electronic states are obtained within the PM3 Hamiltonian with configuration interaction. Structural relaxations are found to reverse the order of 1^1B_{3u} and 2^1A_g with increasing number of *peri*-linked naphthylene repeat units, N. The adiabatic 1^1B_{3u} state is below 2^1A_g for perylene, in line with its strong fluorescence. For terrylene, $S_1 = 2A_g$ and $S_2 = 1B_{3u}$ are nearly degenerate. For N = 4 and 5, $S_1 = 2A_g$ is predicted lower than $1B_{3u}$ by 0.17 and 0.24 eV, respectively. These results explain the decrease of fluorescence quantum yield in *tert*-butyl-substituted oligorylenes, especially on going from terrylene (74%) to quaterylene (5%).

I. Introduction

Oligorylenes have attracted considerable experimental and theoretical efforts since they were synthesized in a succession of well-defined soluble oligomers up to the pentamer.[1] Their photon excitation thresholds[1,2] are lower even than those of polyenes[3] of comparable conjugation length. Both from oligomer extrapolation[1a] and from theoretical assessments,[4−7] the band gap of the polymeric form, polyperinaphthylene (PPN), is expected to be below 1 eV, which is at least 0.5 eV less than for *trans*-polyacetylene (PA). Like polyenes, oligorylenes have two low-lying excited singlet states of odd and even parity.[8,9] The optical absorption spectra of oligorylene radical monoions[8,10] are also similar to those of polyene monoions,[11] and the similarity can be explained in terms of the dominant configurations and π-orbitals involved in the lowest excited doublet states.[8]

Polyenes are a good reference point in discussing the photophysics of oligorylenes because the conjugated skeleton of rylenes can be viewed as two rigidly connected *cis*−*trans* polyene chains.[6,8] The canonical transformation of π-orbitals of oligorylenes into even and odd with respect to the σ_y mirror plane casts the conjugated skeleton into two disjoint extended Hückel graphs (Figure 1). The highest occupied and lowest unoccupied π-orbitals that are essential for the nature of the excited states and the electron−phonon coupling regime belong to the odd manifold for which σ_y is a nodal plane. Consequently, they are delocalized exclusively on the upper and lower peripheries of the rylenic backbone. The periphery itself is a *cis*−*trans* polyene chain of 4N π-sites where *N* is the number of naphthylene repeat units. Hence, with respect to conjugation length, the *N*-rylene oligomer compares to a 4*N* polyene chain.

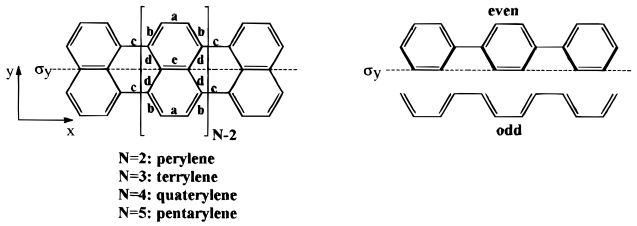

Figure 1. Oligorylenes and the labeling of conjugated CC bonds (left) and Hückel graphs associated with σ_y odd and σ_y even π-orbitals of oligorylenes (right). Bold edges denote Hückel transfer integrals multiplied by $\sqrt{2}$.

The bond alternation of finite polyenes is fixed only by the requirement for terminal double bonds. Similarly, it has been shown[6] that the bond alternation on the periphery of rylenes that can be either *trans*−*cisoid* (benzenoid form) or *cis*−*transoid* (quinoid form)[4,5] is sensitive to boundary conditions. For finite oligorylenes, the aromatic stabilization of the terminal naphthylenes imposes single-bond character on the adjacent *peri*-bonds and fixes a benzenoid structure on the internal repeat units, either. With cyclic boundary conditions this factor is removed. The benzenoid form of PPN is associated with the same number of Kekulé structures as the quinoid one, and the stabilization of either of them is related to the Peierls instability of PA.[12] The Hückel model augmented with $\pi-\sigma$ coupling predicts a slightly quinoid ground-state structure of PPN.[4,6] Yet on a higher level of theory, the benzenoid form of the oligomers is found to persist in the polymer, too.[6] The quinoid form of PPN is predicted to be unstable. However, in contrast to typical nondegenerate polymers such as poly(*p*-phenylene) and poly(*p*-phenylenevinylene) where the alternative double-bond localization is merely a limiting Kekulé structure, the quinoid form of PPN corresponds to the second lowest local minimum of a potential energy surface, which has the shape of an asymmetric double well.[6] That is why PPN can be viewed as a nearly degenerate polymer. Its electron−phonon coupling regime is

* Corresponding author: e-mail karabuna@mbox.digsys.bg; Fax (56)-686141.
† Bourgas University of Technology.
‡ Max-Planck-Institut für Polymerforschung.
§ E-mail baumgart@mpip-mainz.mpg.de; Fax (6131)379100.

S1089-5639(98)01473-X CCC: $15.00
Published on Web 08/11/1998

expected to be weaker than for PA but stronger than for typical nondegenerate polymers. Charged and neutral excitations in polyenes involve strong structural relaxations up to a complete reversal of the bond alternation in the lowest excited $2A_g$ singlet[13] (the spin index for singlet is omitted hereafter). Polaron and exciton relaxations in oligorylenes[8] are not so pronounced but still can locally change the structure of the conjugated backbone toward the quinoid one.

PPP calculations[8] at the ground-state geometry with configuration interaction limited to single and double excitations assign the lowest excited singlet, S_1, of the oligomers from perylene to pentarylene to a dipole-allowed $1B_{3u}$ state of HOMO $\rightarrow$ LUMO parentage. The second excited singlet is a correlated, dipole-forbidden $2A_g$ state that involves both single and double excitations. Nevertheless, on the basis of the relationship of the excitations in rylenes and polyenes, and the drastic drop of fluorescence in quaterylene and pentarylene,[1] it was hypothesized[8] that $2A_g$ might be lower than $1B_{3u}$ for these two oligomers. A generalized quantum-cell model[9] using expanded symmetry-adapted π-sites makes the connection of rylenes to polyenes more explicit. In the correlation limit, it still predicts $S_1 = 1B_{3u}$ for small rylenes up to terrylene ($N = 3$). However, with increasing N, a crossover to $S_1 = 2A_g$ is expected around $N = 4$.

In this paper we report computational results for the three lowest singlets ($1A_g$, $1B_{3u}$, and $2A_g$) of oligorylenes from perylene to pentarylene. The equilibrium geometry for each particular electronic state is separately obtained within the semiempirical PM3[14] model with configuration interaction (CI). At the ground-state minimum geometry, the lowest vertical one-photon transition to $1B_{3u}$ is below the two-photon $2A_g$ threshold for all oligomers studied. Structural changes in the excited electronic states are found to be essential for their relative ordering. They lead to a reversal of the lowest adiabatic excited states of odd and even parity in larger oligomers. We find the adiabatic $2A_g$ state lower than $1B_{3u}$ for terrylene, quaterylene, and pentarylene. Moreover, for pentarylene, the "fixed" $2A_g$ state is predicted to be below $1B_{3u}$ at the $1B_{3u}$ minimum geometry. In line with the lack of fluorescence from pentarylene, this result suggests fast vertical $2A_g \leftarrow 1B_{3u}$ relaxation after the usual one-photon excitation.

II. Computational Methods

Theoretical prediction of excited states is a demanding task because it requires both a reliable quantum chemical Hamiltonian and, in some cases, extended configuration interaction (CI) to reproduce correlated electronic states. The largest oligomer studied herein is pentarylene with 50 carbon π-sites. Such a molecular size is far beyond the domain of applicability of computational techniques at an ab initio level of theory. Indeed, much of the theoretical work[15,16] on correlated excited states in conjugated systems has been done in a π-electronic approximation, often augmented with $\pi-\sigma$ coupling to account for structural relaxations. We have chosen an all-valence electron semiempirical Hamiltonian as a compromise between precision and feasibility. Among the variety of semiempirical models, the two more recent methods, namely, PM3[14] and AM1,[17] have gained ample credit. Whereas their relative advantages may be discussed in general[14] or for a particular molecule,[18] PM3 was picked up for the sake of comparability with previous studies[5,6,8] on the title compounds.

The demand for expanded CI required several upgrades of the MOPAC[19] program package. First, the CI module was advanced to handle up to 64 000 configurations that allow complete CI for 10 electrons in 10 spin-restricted orbitals. The enlarged CI required disk storage of CI integrals and implementation of Davidson's diagonalization technique.[20] To achieve a more efficient geometry optimization for a particular electronic state, the configurational basis can be optionally contracted to a subset of configurations that reproduce a predefined portion of the corresponding exact CI eigenvector. Herein, the geometry optimization was performed by using a CI expansion that covers at least 99.5% of the exact initial CI eigenstate. This allowed us, in the course of geometry optimization, to store and diagonalize the reduced CI matrix directly in memory even in the most severe case. Finally, equilibrium point calculations were performed within the unreduced CI basis.

Oligorylenes were taken to be planar, with D_{2h} point group symmetry. The geometry was optimized in the complete set of Cartesian degrees of freedom under D_{2h} symmetry restrictions. For the sake of simplicity and reliability of the energy minimization, the energy gradient was calculated numerically by using a three-point approximation for each independent coordinate.

For rylenes of D_{2h} symmetry, the π-orbitals delocalized on the periphery belong to b_{3g} and a_u, which are both odd with respect to the σ_z and σ_y mirror planes. The b_{3g} and a_u orbitals are, respectively, even and odd for the σ_x mirror plane. For finite oligorylenes the HOMO is a_u and the LUMO is b_{3g}. In the ground state, the benzenoid form is favored since it stabilizes a_u orbitals and destabilizes b_{3g} ones. The dominant configurations of the lowest excited states involve single and double excitations from a_u HOMOs to b_{3g} LUMOs for $1B_{3u}$ and $2A_g$, respectively. As a consequence, bond localization on the periphery is partially inverted relative to the ground state, and the alternative quinoid form is favored. For the purpose of quantification of the peripheral bond-length alternation of rylenes, a bond-alternation parameter has been introduced previously.[6] It pertains to any *trans*-bond of the peripheral chain with length r_b and has the form $\Delta r_b = {}^1/_2(-r_a + 2r_b - r_c)$, where r_a and r_c are the lengths of the adjacent peripheral *cis*-bonds (see Figure 1). Benzenoid and quinoid bond length distortions are described by negative and positive Δr_b values, respectively. To characterize the prevailing bond-length distortion we use further the average bond alternation, Δr, which is the average of Δr_b for all peripheral *trans*-CC bonds.

Due to computational limitations, it was impractical to perform CI in the complete set of π-orbitals. Still, to obtain comparable results for different oligomers, the size of the CI active space was kept proportional to the oligomeric size. Besides, only b_{3g} and a_u orbitals were taken in the CI expansion since they couple most strongly to the peripheral bond-length distortions. Consequently, for the oligomer of N naphthylene repeat units, the highest N occupied and the lowest N unoccupied orbitals of a_u and b_{3g} symmetry were included in the CI active space.

III. Results and Discussion

A. Equilibrium Geometry. The ground-state equilibrium structure of oligorylenes reflects a benzenoid-like double-bond localization (Figure 2). The comparison with previous PM3 results[5,6] on Hartree−Fock level shows that CI has the effect of reducing bond-length alternation, especially on the periphery of the conjugated skeleton. That CI decreases ground-state bond alternation has been well-established for polyenes.[21] As usual, the dominant configuration of the ground electronic state is the

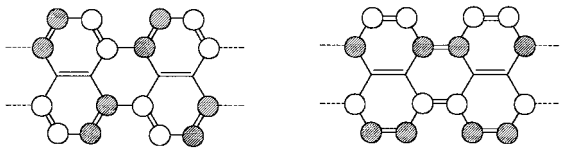

Figure 2. (a) Symmetry of a_u HOMO and benzenoid double-bond localization; (b) Symmetry of b_{3g} LUMO and quinoid double-bond localization.

Hartree−Fock wave function. However, its contribution to the CI expansion decreases in parallel with oligomeric length from 97% for perylene ($N = 2$) to 92% for pentarylene ($N = 5$). The next significant contribution to the ground-state CI wave function comes from the double excitation from HOMO to LUMO, which contributes some quinoid bond localization and, hence, reduces bond alternation. With respect to the dependence of peripheral bond alternation on oligomeric length, N, Δr decreases in magnitude from $\Delta r = -0.050$ Å for perylene to $\Delta r = -0.042$ Å for pentarylene. The predicted reduction of bond alternation for longer rylenes is in line with the increased contribution of the doubly excited configuration to the ground-state eigenfuction.

As expected, bond localization is weaker in the dipole-allowed $1B_{3u}$ singlet (see Figure 3). The relatively longer *peri*-bonds **c** are rather due to through-space repulsion of the peripheral protons at the positions incident to **a** and **b** bonds than to any predominant double-bond localization inherent to the conjugated backbone. Terminal **b** bonds have typical aromatic lengths. Bond length alternation, as described by Δr_b, evolves from benzenoid for the terminal naphthylene units to quinoid for the central ones. Since in Δr the effect of relatively short **a** bonds is canceled by the longer *peri*-bonds **c**, its value is close to zero. The average bond alternation varies from $\Delta r = 0.004$ Å for perylene to $\Delta r = -0.012$ Å for pentarylene.

The $2A_g$ minimum structures correspond to the quinoid form only as far as the peripheral chains have a *cis*−*transoid* double-bond localization. The central **e** bonds on the C_{2x} axis are even depleted of π-electronic density relative to the ground state and have typical single-bond lengths. Aromatic stabilization of the outermost naphthylenes is still effective, especially for the longer rylenes. Indeed, the terminal **b** bonds are gradually shortened on going from perylene (1.421 Å) to pentarylene (1.383 Å). Inverted double-bond localization with short **a** bonds is evident for the central repeat units of pentarylene and quaterylene. The reversal of peripheral bond alternation can be best illustrated by the Δr_b values for pentarylene. Local bond alternation gradually evolves from *trans*−*cisoid* ($\Delta r_b = -0.010$ Å) for the terminal to *cis*−*transoid* ($\Delta r_b = 0.032$ Å) for the central repeat units.

B. Energy of Excited States. Table 1 collects calculated ground- and excited-state energies at different equilibrium geometries. The values are given relative to the ground-state equilibrium energy of the particular oligomer. Minimum energies of the excited states are printed in boldface type and correspond to the adiabatic or 0−0 excitation. Excited-state energies calculated at the ground-state structure equilibrium (first row of each section) correspond to vertical excitation energies. Figure 4 gives adiabatic and vertical excitation energies as a function of reciprocal oligomeric length, $1/N$. The "fixed" $2A_g$ electronic state energy calculated at the $1B_{3u}$ minimum geometry is also given. The dependence of the energy of the different electronic states on the bond-alternation parameter is plotted in Figure 5.

As expected, both adiabatic and vertical excitation energies exhibit a considerable lowering with increasing conjugation length. As seen from Figure 4, excitation energies almost perfectly conform to the linear $1/N$ dependence. In fact, the linear fits on the graph provide correlation coefficients higher than 99.7% for both the adiabatic and vertical excitation energies plotted. Apart from the fundamental arguments[22,23] in support of such a dependence, this feature allows straightforward extrapolation of the excited-state energies to $1/N \rightarrow 0$ for the hypothetical polymer, PPN.

The longest wavelength absorption bands of oligorylenes[1,2] in solution lie considerably lower than the calculated adiabatic or vertical $1A_g \rightarrow 1B_u$ excitations for the whole series. Calculated vertical $1A_g \rightarrow 1B_{3u}$ excitations exceed the position of the absorption maxima by a margin that varies from ∼0.48 eV for perylene to ∼0.59 eV for pentarylene. Such a systematic overestimation of the transition energy is not striking, having in mind the ionic character of the $1B_{3u}$ excited state. On one hand, the position of $1B_{3u}$ should be very sensitive to interaction with solvents; in polyenes, $1B_u$ for the isolated molecule[24] is ∼0.3 eV higher than in matrixes[3] or solvents.[11] On the other hand, extensive theoretical studies on polyenes[25] suggest that the quantitative description of the ionic $1B_u$ state is even more demanding than for the covalent $2A_g$, both with regard to the atomic basis and CI in the $\sigma\pi^*$ space.

The adiabatic $1A_g \rightarrow 1B_{3u}$ excitations are predicted to be about 0.16−0.19 eV lower than the vertical ones. Such large exciton relaxation energies are incompatible with the very small Stokes shifts of ∼ 0.05 eV between absorption and emission bands of substituted perylene, terrylene, and quaterylene in solution.[1] This discrepancy can be partially ascribed to the restricted configuration interaction. Extending the CI active π-orbitals for perylene from 4 to 10 leads to more close equilibrium geometries of $1A_g$ and $1B_{3u}$ and, consequently, to a decrease of $1B_{3u}$ relaxation energy from 0.191 to 0.177 eV. For the purpose of comparison, similar computations were performed for *all-trans*-polyenes of $4N$ carbon sites, which correspond to the peripheral chains of N-rylenes. Calculated $1B_u$ exciton relaxation energy increases from ∼0.20 eV for octatetraene ($N = 2$) to ∼0.24 eV for hexadecaoctaene ($N = 4$), which is comparable with more accurate theoretical results.[25] As expected for the rigid rylenic skeleton, structural relaxations are smaller in oligorylenes than in polyenes of the same conjugation length despite the larger molecular size of the former. Moreover, in contrast to polyenes, $1B_{3u}$ exciton relaxation energies of rylenes are predicted to decrease with conjugation length.

For all oligomers at the ground-state geometry, the "fixed" $2A_g$ state is predicted well above $1B_{3u}$. For perylene, the vertical $1A_g \rightarrow 2A_g$ excitation is obtained ∼0.7 eV higher than the vertical $1A_g \rightarrow 1B_{3u}$ transition. However, both vertical and adiabatic $1A_g \rightarrow 2A_g$ excitation energies decrease faster with oligomeric length than for the dipole-allowed $1B_{3u}$ state. As a result, the extrapolated lowest one- and two-photon vertical excitations become almost degenerate in the polymer limit $1/N \rightarrow 0$.

The structural relaxations of the $2A_g$ exciton are much more pronounced than for $1B_{3u}$. Due to the reversal of peripheral bond-length alternation, the difference between vertical and adiabatic $1A_g \rightarrow 2A_g$ transition energies amounts to more than 0.7 eV on the average. With increasing conjugation length, it decreases from 0.77 eV for perylene to 0.70 eV for pentarylene. For comparison, $2A_g$ relaxation energies of $4N$-site polyenes are calculated to be ∼0.2−0.3 eV larger and increasing with

TABLE 1: Energy of $1A_g$, $1B_{3u}$, and $2A_g$ Electronic States Calculated at Different Minimum Geometries[a]

oligomer (N)	geometry	$E(1A_g)$/eV	$E(1B_{3u})$/eV	$E(1B_{3u})$/eV absorption	$E(2A_g)$/eV	Δr/Å
perylene (2)	$1A_g$	**0.0**	3.337		4.033	−0.050
	$1B_{3u}$	0.160	**3.146**	2.86,[b] 2.82[c]	3.481	0.004
	$2A_g$	0.633	3.356		**3.261**	0.047
terrylene (3)	$1A_g$	**0.0**	2.774		3.252	−0.045
	$1B_{3u}$	0.139	**2.610**	2.21,[b] 2.22[c]	2.758	−0.004
	$2A_g$	0.573	2.809		**2.552**	0.035
quaterylene (4)	$1A_g$	**0.0**	2.454		2.807	−0.043
	$1B_{3u}$	0.129	**2.300**	1.85,[b] 1.88[c]	2.316	−0.010
	$2A_g$	0.522	2.637		**2.124**	0.027
pentarylene (5)	$1A_g$	**0.0**	2.253		2.552	−0.042
	$1B_{3u}$	0.120	**2.094**	1.66[c]	2.052	−0.013
	$2A_g$	0.516	2.262		**1.853**	0.020

[a] Values are given relative to the ground-state equilibrium. Numbers in boldface correspond to the adiabatic excitation energies. The longest wavelength optical absorption maxima are also given. [b] From ref 2. [c] From ref 1a. In the rightmost column, the average bond-alternation parameter for the particular minimum-energy structure is given.

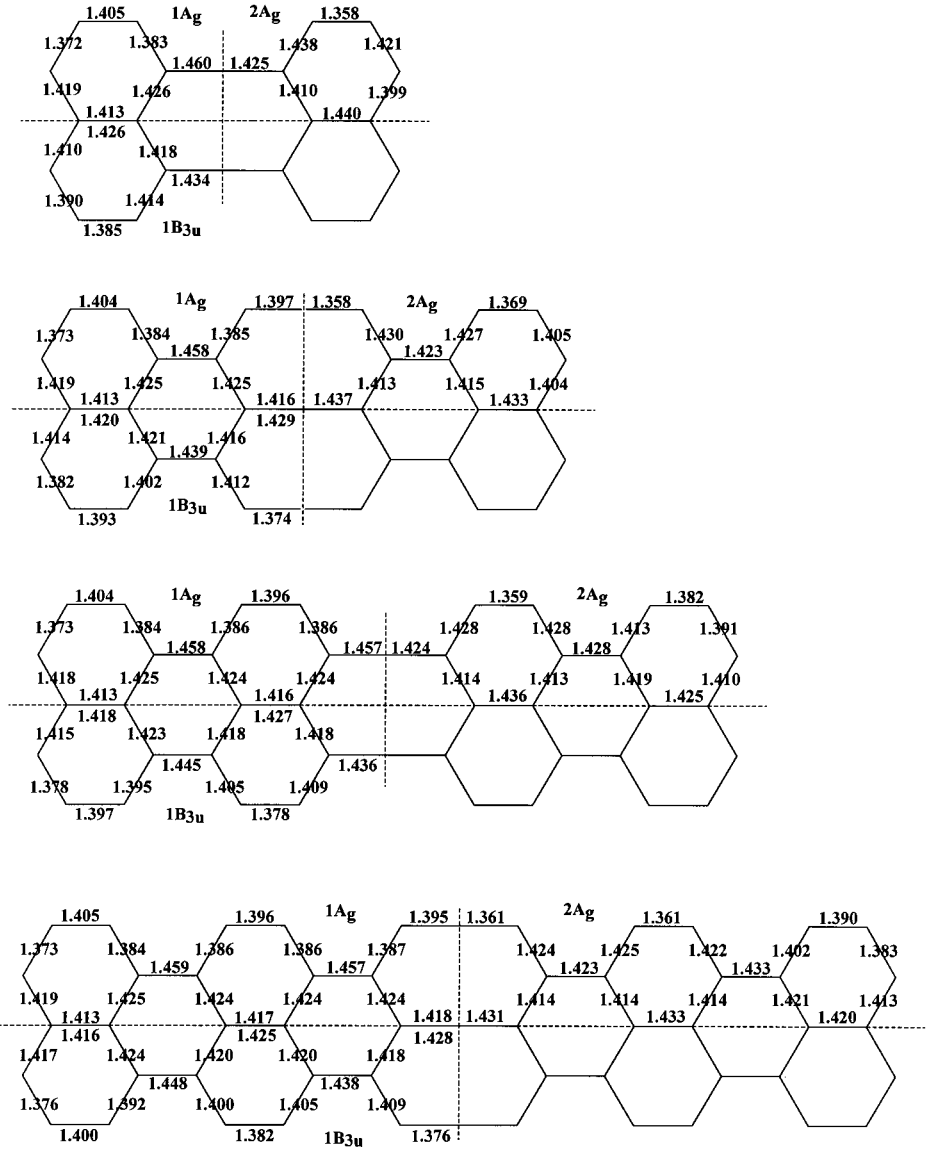

Figure 3. CC bond lengths of D_{2h} oligorylenes at the energy minimum in ground and excited electronic states: $1A_g$, top left; $1B_{3u}$, bottom left; $2A_g$, top right.

conjugation length on both the present semiempirical and ab initio level of theory.[25]

For perylene, the adiabatic $2A_g$ energy is higher than $1B_{3u}$ by 0.12 eV. First, for terrylene the relaxed $2A_g$ state is predicted to be below the $1B_{3u}$ minimum by a marginal 0.058 eV. The crossover to an even-parity S_1 is more distinct for quaterylene and pentarylene, where equilibrium $E(1B_u) - E(2A_g)$ increases to 0.176 and 0.241 eV, respectively. In general, $2A_g$ excitation energies exhibit a steeper slope as a function of $1/N$ than for $1B_{3u}$. Extrapolated $1B_{3u}$ adiabatic energies suggest a relaxed

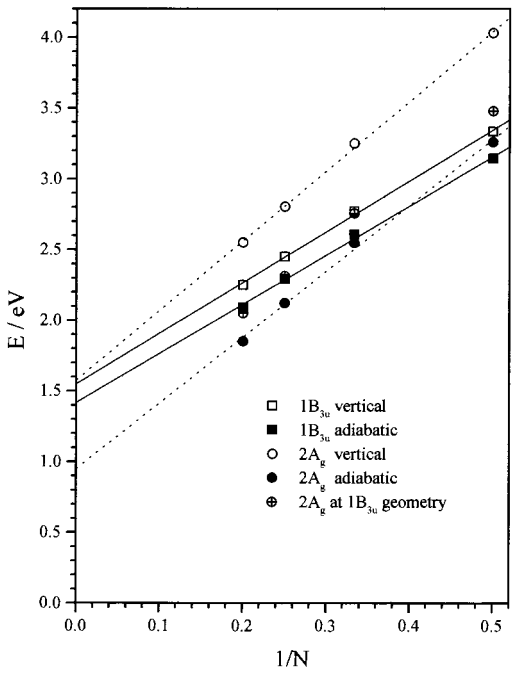

Figure 4. Calculated vertical and adiabatic energies of $1B_{3u}$ and $2A_g$ as a function of reciprocal oligomeric length $1/N$. The $2A_g$ state energy at $1B_{3u}$ minimum geometry is also given.

odd-parity exciton at around 1.4 eV for the polymer, whereas the relaxed even-parity state is expected some 0.45 eV lower. Because of the faster decrease of $2A_g$ energies with N, the "fixed" $2A_g$ electronic state drops below $1B_{3u}$ equilibrium for pentarylene.

The ordering of excited states predicted in the calculation is in good agreement with the fluorescence of *tert*-butyl-substituted oligorylenes.[1] According to Kasha's rule,[26] fluorescence occurs from the lowest excited singlet S_1. For perylene this is definitely the dipole-allowed $1B_{3u}$ and fluorescence is strong. Fluorescence quantum yield decreases from 94% to 70% for substituted terrylene and drops further to a surprisingly low 5% in quaterylene. Accordingly, we predict almost degenerate S_1 and S_2 states of even and odd parity in terrylene, and a $2A_g$ exciton definitely lower in energy than the dipole-allowed $1B_{3u}$ state in quaterylene. Hence, the most probable mechanism of fluorescence quenching is an internal $2A_g \leftarrow 1B_{3u}$ adiabatic conversion, followed by a radiationless relaxation to the ground state. In pentarylene no measurable fluorescence is observed. Pentarylene is the first oligomer of the series for which a more efficient vertical pathway for decay of the $1B_{3u}$ exciton is predicted since the potential energy surface of $2A_g$ is below the $1B_{3u}$ minimum (see Figure 5).

IV. Conclusions

The calculations performed confirm at a quantitative level that a crossover to an even-parity S_1 takes place in rylenes with more than 3 naphthylene repeat units. The reversal of the odd- and even-parity excitons clarifies the drastic decrease of fluorescence efficiency on going from terrylene to quaterylene. From a theoretical aspect, this finding can be traced back to the topology of the rylenic skeleton, which is related to that of polyenes. The frontier π-orbitals of an N-rylene expand on two disjointed peripheral conjugated chains of $4N$ π-sites. Because of the enhanced coupling of π-electrons to bond-length alternation, typical for polyenes, the rylenic skeleton, despite its *peri*-condensed nature, is still susceptible to structural changes upon photoexcitation. That is why we find both electron correlation and exciton relaxation equally important for the description of the excited states. Namely, the crossover to an even-parity S_1 in longer rylenes that can be deduced from the observed fluorescence quenching and general theoretical arguments is

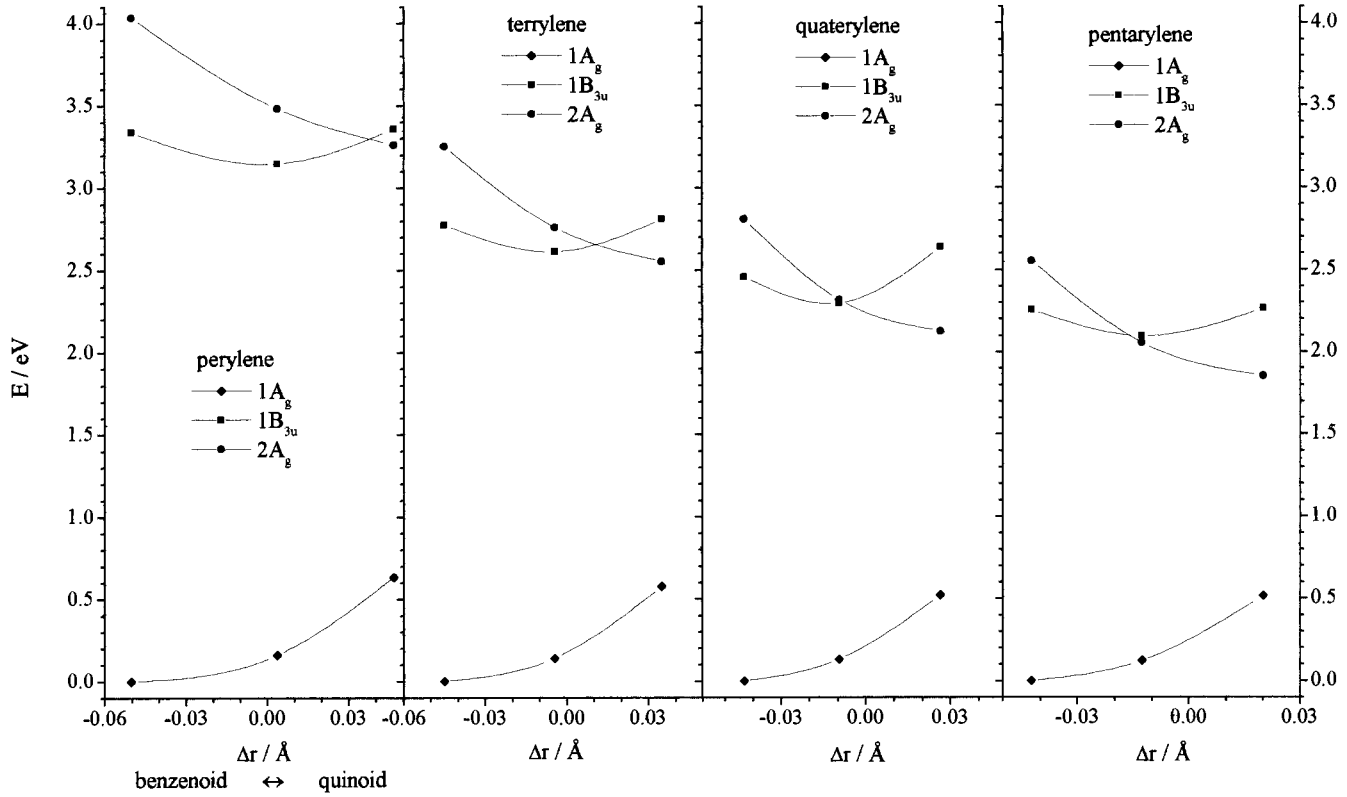

Figure 5. Potential energies of the ground and excited states as a function of the bond-length alternation parameter. The curves are only a guide for the eye.

reproduced in the quantum chemical calculation only when relaxed, adiabatic excited states are considered.

The comparison with excitation/emission spectra of substituted oligorylenes indicates, however, that the semiempirical method used tends to overestimate one-photon excitation energies and structural relaxations. This drawback can be partially repaired by extending the configuration interaction, but this could be inherent to the semiempirical Hamiltonian, as well. Because of these deficiencies, it is unrealistic to predict exactly whether the crossover from an odd-parity to an even-parity S_1 takes place in terrylene or quaterylene. Besides, as mentioned already, the position of the ionic $1B_{3u}$ state can be very sensitive to solvent−solute interactions and polarization effects. In any case, the reversal of the symmetry of S_1 and S_2 occurs for much larger conjugation length than in polyenes: quaterylene compares to a 16 π-site chain, whereas $S_1 = 2A_g$ already in hexatriene and probably in butadiene. Parallel computations for polyenes with the same method illustrate the difference between rylenes and polyenes. First, the electron correlation in rylenes is reduced because the extended π-orbitals are more diffuse involving two, instead of one, conjugated chain. Next, because of the aromatic stability of the naphthylene subunits, exciton relaxations are much weaker. In view of the fact that such a conjugation-length-dependent reversal of S_1 and S_2 is not typical for oligomers of nondegenerate conjugated polymers, the more detailed description of $1B_{3u}$ and $2A_g$ in quaterylene and pentarylene remains a challenge, from both theoretical and experimental aspects.

Acknowledgment. One of the authors (S.K.) thanks the Alexander von Humboldt-Stifftung for the donation of the work station, HP 9000 Model C100, on which the quantum chemical calculations were done. The study was supported by Grant X-606 of the Bulgarian Ministry of Education and Science.

References and Notes

(1) Koch, K.-H.; Müllen, K. *Chem. Ber.* **1991**, *124*, 2091. (b) Bohnen, A.; Koch, K.-H.; Lüttke, W.; Müllen, K. *Angew. Chem., Int. Ed. Engl.* **1990**, *29*, 525.

(2) Clar, E. *Polycyclic Hydrocarbons*; Academic: London, 1964; Vol. 2.

(3) Hudson, B. S.; Kohler, B. E.; Schulten, K. In *Excited States*; Lim, E., Ed.; Academic: New York, 1982; Vol. 6, p 1. Kohler, B. E.; Sprangler, C.; Westerfield, C. *J. Chem. Phys.* **1988**, *89*, 5422. D'Amico, K. L.; Manos, C.; Christensen, R. L. *J. Am. Chem. Soc.* **1980**, *102*, 1777.

(4) Brédas, J. L.; Baughman, R. H. *J. Chem. Phys.* **1985**, *83*, 1316.

(5) Viruela-Martin, R.; Viruela-Martin, P. M.; Orti, E. *J. Chem. Phys.* **1992**, *97*, 8470.

(6) Karabunarliev, S.; Baumgarten, M.; Müllen, K.; Tyutyulkov, N. *Chem. Phys.* **1994**, *179*, 421.

(7) Tyutyulkov, N.; Tadjer, A.; Mintcheva, I. *Synth. Metals* **1990**, *38*, 313.

(8) Karabunarliev, S.; Gherghel, L.; Koch, K.-H.; Baumgarten, M. *Chem. Phys.* **1994**, *189*, 53.

(9) Soos, Z. G.; Hennessy, M. H.; Wen, G. *Chem. Phys. Lett.* **1997**, *274*, 189.

(10) Baumgarten, M.; Koch, K.-H.; Müllen, K. *J. Am. Chem. Soc.* **1994**, *116*, 7341.

(11) Bally, T.; Roth, K.; Tang, W.; Schrock, R.; Knoll, K.; Park, L. Y. *J. Am. Chem. Soc.* **1992**, *114*, 2440.

(12) Klein, D. J.; Schmalz, T. G.; Seitz, W. A.; Hite, G. E. *Int. J. Quantum Chem.* **1986,** *S19*, 707. Seitz, W. A.; Schmalz, T. G. In *Valence Bond Theory and Chemical Structure*; Klein, D. J., Trinajstic, N., Eds.; Elsevier: Amsterdam, 1990; p 525.

(13) Aoyagi, M.; Ohmine, I.; Kohler, B. E. *J. Phys. Chem.* **1990**, *94*, 3922.

(14) Stewart, J. J. P. *J. Comput. Chem.* **1989**, *10*, 209 and 221.

(15) Soos, Z. G.; Galvão, D. S.; Etemad, S. *Adv. Mater.* **1994**, *6*, 280. Soos, Z. G.; Ramasesha, S.; Galvão, D. S.; Kepler, R. G.; Etemad, S. *Synth. Metals* **1993**, *54*, 35.

(16) Orlandi, G.; Zerbetto, F.; Zgierski, M. Z. *Chem. Rev.* **1991**, *91*, 867, and references therein.

(17) Dewar, M. J. S.; Zoebish, E. G.; Healy, E. F.; Stewart, J. J. P. *J. Am. Chem. Soc.* **1985**, *107*, 3902.

(18) See for instance: (a) Lhost, O.; Brédas, J. L. *J. Chem. Phys.* **1992**, *96*, 5279. (b) Galvão, D. S.; Soos, Z. G.; Ramasesha, S.; Etemad, S. *J. Chem. Phys.* **1993**, *98*, 3016.

(19) Stewart, J. J. P. *MOPAC: A General Molecular Orbital Package* (Version 7.2); Quantum Chemistry Program Exchange, 1995.

(20) Davidson, E. R. *J. Comput. Phys.* **1975**, *17*, 87. Weber, J.; Lacroix, R.; Wanner, G. *Comput. Chem.* **1980**, *4*, 55. Cisneros G.; Bunge, C. F. *Comput. Chem.* **1984**, *8*, 157.

(21) Kofranek, M.; Lischka, H.; Karpfen, A. *J. Chem. Phys.* **1992**, *96*, 982. Choi, C. H.; Kertesz, M.; Karpfen, A. *J. Chem. Phys.* **1997**, *107*, 6712.

(22) Brédas, J. L.; Silbey, R.; Boudreux, D.; Chance, R. R. *J. Am. Chem. Soc.* **1983**, *105*, 6555.

(23) Deussen, M.; Bässler, H. *Chem. Phys.* **1992**, *164*, 247.

(24) Leopold, D. G.; Pendley, R. D.; Roebber, J. L.; Hemley, R. J.; Vaida, V. *J. Chem. Phys.* **1984**, *81*, 4281. Leopold, G.; Vaida, V.; Granville, M. F. *J. Chem. Phys.* **1984**, *81*, 4210.

(25) Cave R. J.; Davidson, E. R. *J. Phys. Chem.* **1987**, *91*, 4481. Cave R. J.; Davidson, E. R. *J. Phys. Chem.* **1988**, *92*, 614 and 2173.

(26) Kasha, M. *Discuss. Faraday Soc.* **1950**, *9*, 14.